

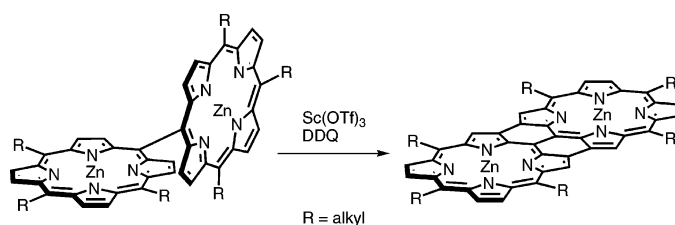
meso-Alkyl-Substituted meso-meso Linked Diporphyrins and meso-Alkyl-Substituted meso-meso, β - β , β - β Triply Linked Diporphyrins

Satoru Hiroto and Atsuhiko Osuka*

Department of Chemistry, Graduate School of Science, Kyoto University, and CREST (Core Research for Evolutional Science and Technology) of Japan Science and Technology Agency (JST), Sakyo-ku, Kyoto 606-8502, Japan

osuka@kuchem.kyoto-u.ac.jp

Received February 3, 2005



AgPF₆-promoted oxidation of 5,10,15-trialkyl zinc(II) porphyrins led to formation of meso-meso linked diporphyrins, which were further oxidized with Sc(OTf)₃ and DDQ to give meso-meso, β - β , β - β triply linked diporphyrins that exhibited a stronger aggregation propensity than corresponding meso-aryl diporphyrins.

Introduction

Covalently linked porphyrin oligomers have been used in molecular devices designed for energy and electron transfer, multiredox catalysis, sensors, and nonlinear optical materials.¹ Electronic interaction among the constituent porphyrins is a key factor that influences the functions and properties of molecules. In the course of these studies, a variety of conjugated porphyrin arrays have been developed, showing that the optical and electrochemical properties of porphyrin oligomers can be tailored to suit a particular application by modifications at the periphery, the central metal, and the mode of conjugation.² Among these, we developed directly meso-meso linked porphyrin oligomers³ and meso-meso, β - β , β - β triply linked porphyrin oligomers.⁴ Electronic conjugation

is almost disrupted in the former oligomers due to perpendicular conformations, but is fully extended over the whole arrays in the latter oligomers, which results in extremely low-energy electronic absorption bands that reach into an infrared region. Recently, large planar molecules with highly conjugated π -network have attracted considerable interest as charge transport layers in photovoltaic cells (PVC) and field-effect transistors (FET).⁵ It is known that the particular suitability for these applications relies on the self-assembling ability to form columnar stacks which facilitate the one-dimensional charge transport.

In the previous studies, we employed 5,15-bis(3,5-*tert*-butylphenyl)-substituted zinc(II) porphyrin as a build-

(1) (a) Wasielewski, M. R. *Chem. Rev.* **1992**, *92*, 435. (b) Gust, D.; Moore, T. A.; Moore, A. L. *Acc. Chem. Res.* **2001**, *34*, 40. (c) Holten, D.; Bocian, D. F.; Lindsey, J. S. *Acc. Chem. Res.* **2002**, *35*, 57. (d) Burrell, A. K.; Officer, D. L.; Plieger, P. G.; Reid, D. C. W. *Chem. Rev.* **2001**, *101*, 2751. (e) Aratani, N.; Osuka, A.; Cho, H. S.; Kim, D. *J. Photochem. Photobiol. C* **2002**, *3*, 25. (f) Yeow, E. K. L.; Ghiggino, K. P.; Reek, J. N. H.; Crossley, M. J.; Bosman, A. W.; Schenning, A. P. H. J.; Meijer, E. W. *J. Phys. Chem. B* **2000**, *104*, 2596. (g) Choi, M.-S.; Yamazaki, T.; Yamazaki, I.; Aida, T. *Angew. Chem., Int. Ed.* **2004**, *43*, 150.

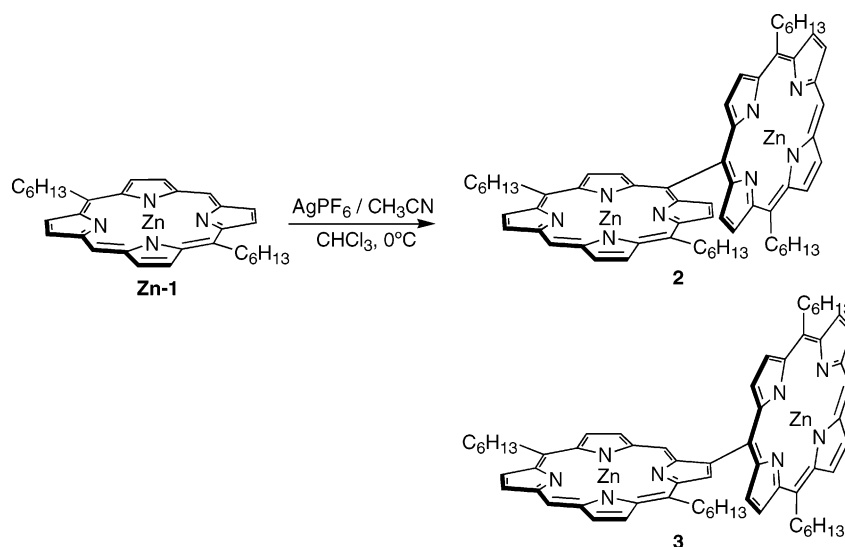
(2) (a) Lin, V. S.-Y.; DiMagno, S. G.; Therien, M. J. *Science* **1994**, *264*, 1105. (b) Crossley, M. J.; Govenlock, L. J.; Prashar, J. K. *Chem. Commun.* **1995**, 2379. (c) Burrell, A. K.; Officer, D. L. *Synlett* **1998**, 1297. (d) Vicente, M. G. H.; Jaquinod, L.; Smith, K. M. *Chem. Commun.* **1999**, 1771. (e) Anderson, H. L. *Chem. Commun.* **1999**, 2323. (f) Sugiura, K.; Fujimoto, Y.; Sakata, Y. *Chem. Commun.* **2000**, 1105. (g) Ogawa, K.; Zhang, T.; Yoshihara, K.; Kobuke, Y. *J. Am. Chem. Soc.* **2002**, *124*, 22.

(3) (a) Osuka, A.; Shimidzu, H. *Angew. Chem., Int. Ed. Engl.* **1997**, *36*, 135. (b) Nakano, A.; Osuka, A.; Yamazaki, I.; Yamazaki, T.; Nishimura, Y. *Angew. Chem., Int. Ed.* **1998**, *37*, 3023. (c) Aratani, N.; Osuka, A.; Kim, Y. H.; Jeong, D. H.; Kim, D. *Angew. Chem., Int. Ed.* **2000**, *39*, 1458.

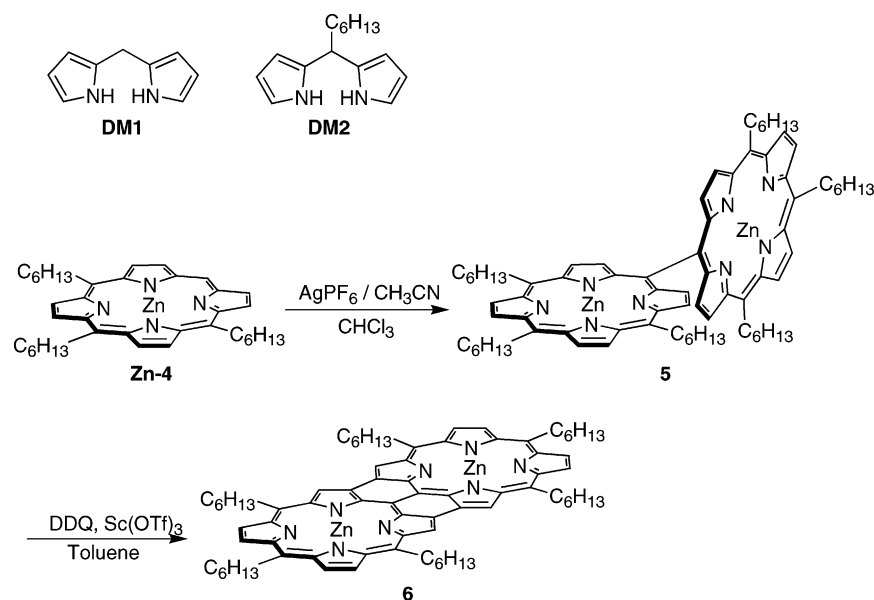
(4) (a) Tsuda, A.; Furuta, H.; Osuka, A. *Angew. Chem., Int. Ed.* **2000**, *39*, 2549. (b) Tsuda, A.; Furuta, H.; Osuka, A. *J. Am. Chem. Soc.* **2001**, *123*, 10304. (c) Tsuda, A.; Osuka, A. *Science* **2001**, *293*, 79. (d) Bonifazi, D.; Scholl, M.; Song, F.; Echegoyen, L.; Accorsi, G.; Armaroli, N.; Diederich, F. *Angew. Chem., Int. Ed.* **2003**, *42*, 4966. (e) Blake, L. M.; Krivokapic, A.; Katterle, M.; Anderson, H. L. *Chem. Commun.* **2002**, 1662.

(5) (a) Garnier, F. *Acc. Chem. Res.* **1999**, *32*, 209. (b) Katz, H. E.; Bao, Z.; Gilat, S. L. *Acc. Chem. Res.* **2001**, *34*, 359. (c) Schmidt-Mende, L.; Fechtenkötter, A.; Müllen, K.; Moons, E.; Friend, R. H.; MacKenzie, J. D. *Science* **2001**, *293*, 1119. (d) Hill, J. P.; Jin, W.; Losaka, A.; Fukushima, T.; Ichihara, H.; Shimomura, T.; Ito, K.; Hashizume, T.; Ishii, N.; Aida, T. *Science* **2004**, *304*, 1481.

SCHEME 1



SCHEME 2



ing block for the purpose of rendering oligomeric porphyrin products soluble enough for manipulations and characterizations, since such a bulky *meso* substituent prevents π - π stacking of porphyrins. To enhance the self-assembling nature by π - π stacking, we thought to replace bulky aryl substituents at the *meso* positions by alkyl substituents.

Results and Discussion

Preparations of *meso*-hexyl porphyrin monomer were performed by the Lindsey method.⁶ Acid-catalyzed condensation of *meso*-free dipyrromethane **DM1** and heptanal followed by oxidation with 2,3-dichloro-5,6-dicyano-1,4-benzoquinone (DDQ) gave 5,15-dihexylporphyrin **1** in 20% yield. Metalation with $Zn(OAc)_2 \cdot 2H_2O$ in refluxing $CHCl_3$ afforded **Zn-1** quantitatively. Then the porphyrin **Zn-1** was subjected to oxidation with $AgPF_6$ in $CHCl_3$ at

$0^\circ C$ for 2 h. After the usual workup, a diporphyrin fraction separated by size exclusion column chromatography (SEC) in 6% yield was found to contain *meso-meso* linked diporphyrin **2** and *meso- β* linked porphyrin dimer **3** in a ratio of 4.5:1 as determined by 1H NMR analysis. Due to the low solubility of the dimers, it was quite difficult to separate **2** and **3**. Then, we changed a substrate to 5,10,15-trihexylporphyrin **4**, which was prepared in 8% yield by the acid-catalyzed condensation of *meso*-free dipyrromethane **DM1**, *meso*-hexyl dipyrromethane **DM2**, and heptanal followed by oxidation with DDQ. This porphyrin can be similarly metalated with $Zn(OAc)_2 \cdot 2H_2O$ to give zinc(II)-porphyrin **Zn-4**. Interestingly, oxidation of **Zn-4** with 1.2 equiv of $AgPF_6$ afforded exclusively *meso-meso* linked diporphyrin **5** in 67% yield. The diporphyrin **5** exhibited its parent ion peak at m/z 1250.6211 (calcd for $C_{76}H_{94}N_8Zn_2$ 1250.6158) in the high-resolution electron-spray-ionization (ESI) mass spectrum and its 1H NMR spectrum showed the peripheral β -protons as four doublets at 8.08, 9.21, 9.61, and 9.65 ppm

(6) Lee, C.-H.; Lindsey, J. S. *Tetrahedron* **1994**, *50*, 11427.

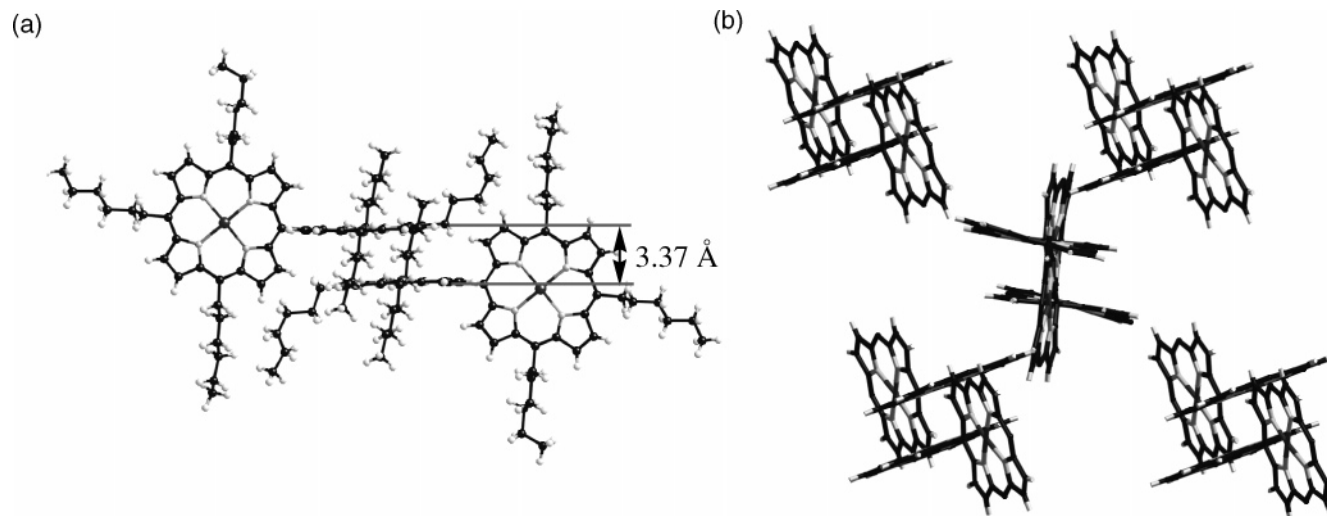


FIGURE 1. (a) A packing structure of one pair of diporphyrins of the two crystallographically independent pairs seen in the solid-state structure of **5**. (b) Packing diagram for **5**.

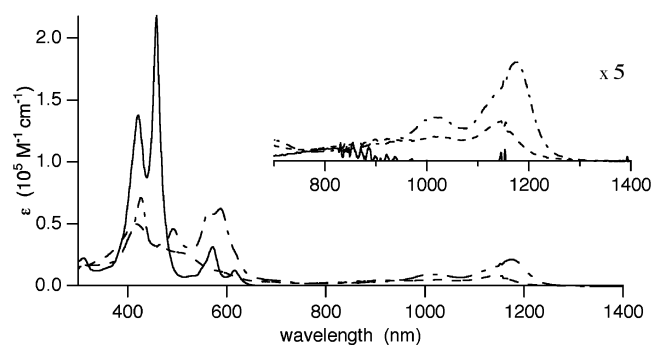


FIGURE 2. Absorption spectra of **5** (—), **6** (---) in CHCl_3 , and **6** in CHCl_3 containing 5% butylamine (- - -).

which are consistent with its symmetric structure. Further, the structure of **5** has been elucidated by X-ray diffraction analysis on its single crystals obtained by slow diffusion of acetonitrile into its chloroform solution (Figure 1).⁷ Similar to the structure of *meso*-aryl-substituted *meso-meso* linked diporphyrin,^{4a} the two porphyrin rings are held almost perpendicularly with a *meso-meso* bond distance of 1.53 Å and a dihedral angle of 87°. Interestingly, in the solid state, two molecules of **5** are paired in a face-to-face arrangement with an interplanar distance of 3.37 Å (Figure 1). The improvement in the coupling regiochemistry (*meso-meso* versus *meso-β*) from **Zn-1** to **Zn-4** is noteworthy. The coupling regioselectivity can be accounted for in terms of the HOMO orbital of the cation radical formed in the oxidation of zinc(II) porphyrin with Ag(I) ion: namely, a_{1u} for *meso-β* and a_{2u} for *meso-meso* coupling, since the a_{2u} orbital has a large spin density at the *meso*-carbons and the a_{1u} orbital has a node at the *meso*-carbons but a substantial spin density at the β -carbons. Therefore, the regioselectivity change from **Zn-1** to **Zn-4** may be ac-

(7) Crystallographic data of *meso*-hexyl *meso-meso* linked diporphyrin: $\text{C}_{153}\text{H}_{189}\text{N}_{16}\text{Zn}_4\text{Cl}_3$, $M_w = 2620.12$, triclinic, space group $P\bar{1}$ (No. 2), $a = 17.51(2)$ Å, $b = 17.69(2)$ Å, $c = 23.43(2)$ Å, $\alpha = 105.17(7)^\circ$, $\beta = 93.96(9)^\circ$, $\gamma = 103.58(9)^\circ$, $V = 6744(11)$ Å³, $D_c = 1.290$ g/cm³, $Z = 2$, $R = 0.096$, R_w (all data) = 0.257, GOF = 1.369 ($I > 2.0\sigma(I)$).

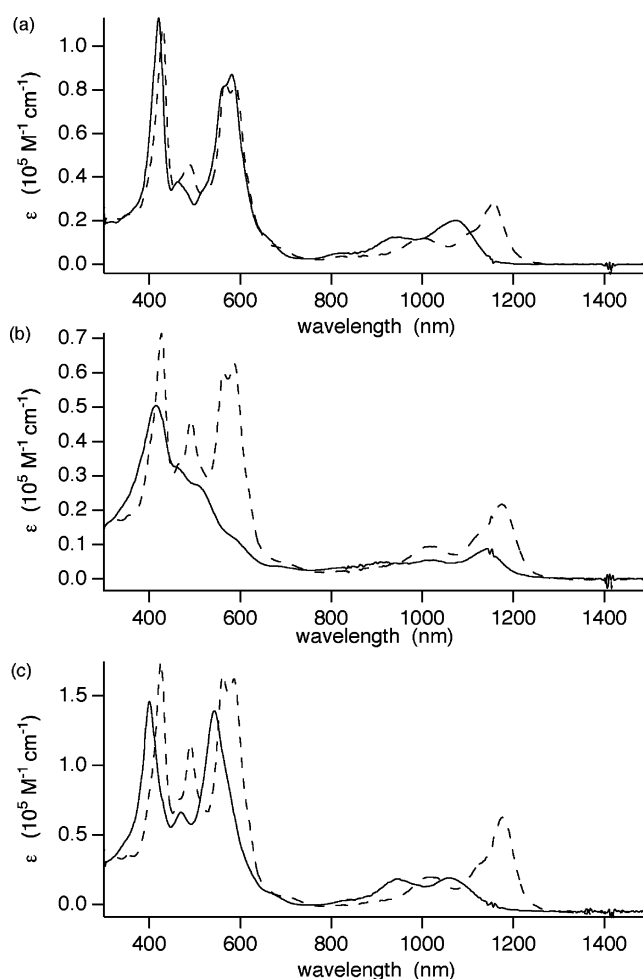
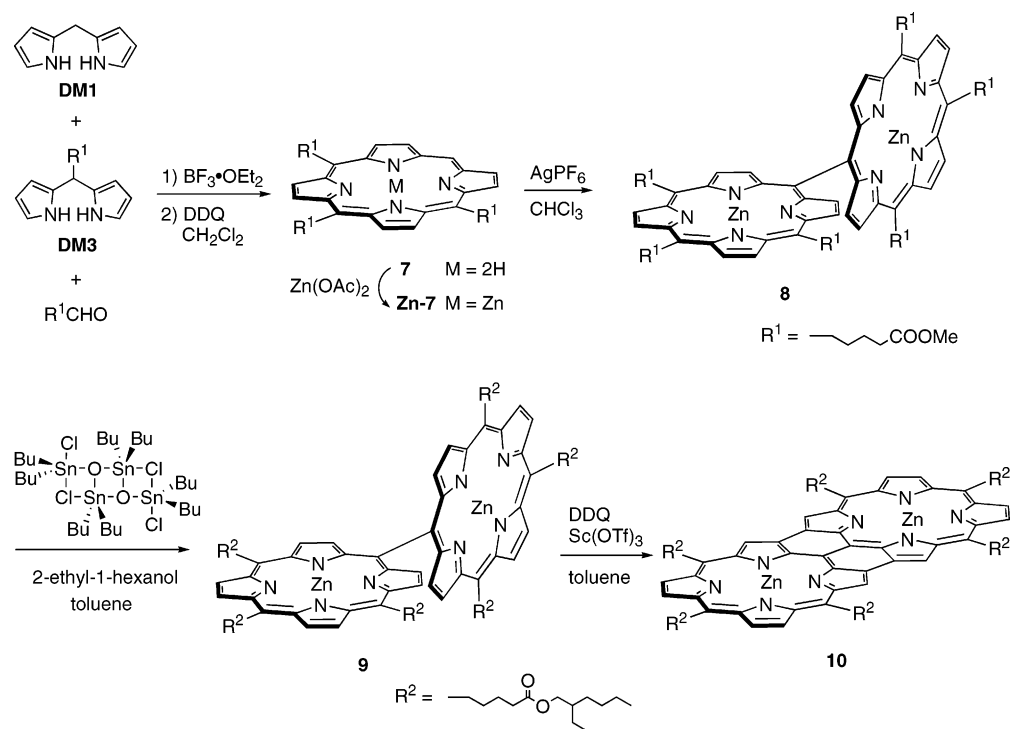


FIGURE 3. Absorption spectra of (a) **13** (b) **6** and (c) **10** in CHCl_3 (—) and in CHCl_3 containing 5% butylamine (---).

counted for as follows: in the case of **Zn-1**, the a_{1u} and a_{2u} orbitals may be close in energy as judged from the formation of **2** and **3**, but an additional attachment of an electron-donating hexyl group at the 10-position in **Zn-4** destabilizes the a_{2u} orbital with respect to the a_{1u} orbital,

SCHEME 3



thus rendering the a_{2u} orbital to be HOMO. This situation may lead to the observed exclusive formation of **5**.

In the next step, the oxidation of **5** with DDQ and Sc(OTf)_3 (5 equiv each) under refluxing conditions for 30 min^{4b} followed by SEC chromatography afforded *meso-meso*, β - β , β - β triply linked diporphyrin **6** as pale red solids in 14% yield. When this reaction was performed with 5 equiv of DDQ and 7 equiv of Sc(OTf)_3 for 12 h at 50 °C, the yield of **6** was improved to 61%. Although **5** is rather soluble in most organic solvents, **6** is practically insoluble in noncoordinating organic solvents such as benzene, CH_2Cl_2 , and CHCl_3 . The triply linked diporphyrin **6** showed its parent ion peak at m/z 1246.5855 (calcd for $\text{C}_{76}\text{H}_{90}\text{N}_8\text{Zn}$ 1246.5845). The ^1H NMR spectrum of **6** in CDCl_3 was too broad to record the chemical shifts but became readable in strongly coordinating pyridine- d_5 , exhibiting the peripheral β -protons at 8.37 ppm as a singlet and at 8.55 and 8.60 ppm as two doublets with $J = 4.6$ Hz. Compound **6** turned out to be too insoluble to perform further manipulations. So we thought to introduce ester groups in the side chains to improve the solubility of triply linked diporphyrins. We chose methyl 6-oxohexanoate as a starting aldehyde that was synthesized very easily from commercially available ϵ -caprolactone. 5,10,15-Tris(4-methoxycarbonylbutyl)porphyrin **7** was prepared in 8% isolated yield by the acid-catalyzed condensation of two different dipyrromethanes, **DM1** and **DM3**, and methyl 6-oxohexanoate. Oxidation of **Zn-7** with 1.2 equiv of AgPF_6 gave *meso-meso* linked diporphyrin **8** in 60% yield. This product has six methyl ester groups that are exchangeable by transesterification. We used a distannoxane catalyst reported by Otera et al. as a mild and effective catalyst for transesterification.⁸ To

enhance the solubility, we performed transesterification with 2-ethyl-1-hexanol for 5 days to give **9** in 80% yield. The oxidation of **9** with 5 equiv of DDQ and 7 equiv of Sc(OTf)_3 at 50 °C followed by SEC chromatography afforded *meso-meso*, β - β , β - β triply linked diporphyrin **10** in 38% yield. It is worthy to note that **10** is soluble enough in CH_2Cl_2 to allow its easy manipulations. The triply linked diporphyrin **10** showed its parent ion peak at m/z 2016.0963 (calcd for $\text{C}_{118}\text{H}_{163}\text{N}_8\text{O}_{12}\text{Zn}_2$ 2016.0969). The ^1H NMR spectrum of **10** in CDCl_3 was broad but analyzable. Addition of a small amount of butylamine made the spectrum sharper with a concurrent downfield-shift of the peaks of the peripheral β -protons from 7.54, 7.73, and 7.83 ppm to 7.71, 8.15, and 8.19 ppm, respectively. Figure 2 shows the absorption spectra of **5** and **6** in CHCl_3 . The *meso-meso* linked zinc(II)-diporphyrin **5** exhibits characteristic split Soret bands at 421 and 458 nm and Q-bands at 572 and 616 nm. The relative intensity of the low-energy Soret band with respect to that of the high-energy Soret band is higher in **5** in comparison to the corresponding *meso*-aryl-substituted *meso-meso* linked zinc(II)-diporphyrins.³ In contrast, the flat zinc(II)-diporphyrin **6** is only slightly soluble in CHCl_3 due to stronger aggregation nature. The resultant absorption spectrum of **6** shows a very broad and blue-shifted Soret band, which suggests π - π stacked pigments. Upon addition of butylamine, this broad absorption spectrum was changed to a split Soret band at 425, 490, and 586 nm and red-shifted and enhanced Q-bands at 1025 and 1174 nm that are typical for *meso-meso*, β - β , β - β triply linked zinc(II)-diporphyrins.⁴ Therefore, these spectral changes can be interpreted as butylamine-induced dissociation through butylamine-zinc(II) center coordination interaction. A similar absorption spectrum for dissociated **6** was observed in THF.

(8) (a) Otera, J.; Danoh N.; Nozaki, H. *J. Org. Chem.* **1991**, *56*, 5307.
 (b) Ohashi, A.; Satake, A.; Kobuke, Y. *Bull. Chem. Soc. Jpn.* **2004**, *77*, 365.

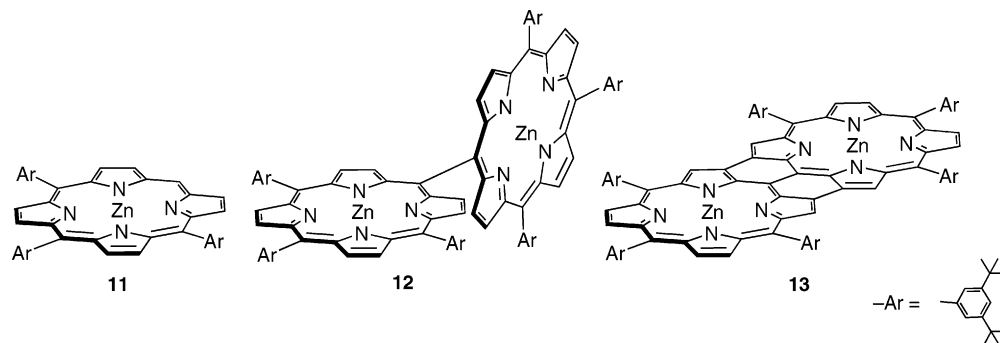


FIGURE 4. *meso*-Aryl-substituted porphyrins.

Figure 3 shows the comparisons of the absorption spectra of **13**, **6**, and **10** in CHCl_3 and CHCl_3 containing 5% butylamine. In the case of *meso*-aryl-substituted triply linked dimer **13**, two strong absorption bands are observed at 420 and 582 nm and broad Q-band-like bands at 949 and 1074 nm in CHCl_3 as reported previously.⁴ Upon addition of butylamine, the strong absorption bands remain nearly at the same positions but the Q-band-like absorption bands are shifted to the low-energy side at 994 and 1155 nm with distinct sharpening. The resultant Q-band-like absorption band shape is reminiscent of those of the zinc(II)-porphyrin monomer that consist of 0–1 and 0–0 vibrational bands. These spectral changes may be ascribed to butylamine-induced disaggregation of somewhat stacked aggregates of **13**. In sharp contrast, the absorption spectrum of **6** in CHCl_3 is very broad, suggesting extensive stacking. Even in the case of **6**, the addition of a small amount of butylamine recovers the typical absorption spectrum characteristic of a triply linked diporphyrin with bands at 426, 561, 1026, and 1179 nm. Notably, both the Soret-like bands and Q-band-like bands are observed approximately at the same positions of the disaggregated **13**. While the absorption spectrum of the ester-bearing triply linked diporphyrin **10** taken after the addition of butylamine is similar to those of disaggregated **13** and **6**, the diporphyrin **10** exhibits unique spectral features in CHCl_3 that are different from those of either **13** or **6**. The absorption spectrum of **10** is not so broad but the Soret-like bands are distinctly red-shifted and the relative intensity of the vibrational bands in the Q-band-like band is different from that of **13**. On the basis of these facts, somewhat ordered aggregated structures are suggested for **10** in nonpolar solvent, which is driven by combined interactions of planar porphyrin π -planes and ester side chains, despite the substantial solubility in CHCl_3 .

The oxidation potentials that were measured by cyclic voltammetry in THF containing 0.1 M Bu_4NPF_6 as a supporting electrolyte are shown in Table 1, where the data of *meso*-aryl compounds **11**, **12**, and **13**^{4b} are also included for comparison. The monomer **Zn-4** underwent a reversible first oxidation at 0.19 V with respect to the ferrocene/ferrocenium ion, which was lower than that of **11** (0.38 V), indicating the elevation of the HOMO orbital by the electron-donating substituents at *meso*-positions. Similar trends were observed for **5**, **6**, **8**, and **10**. The triply linked diporphyrins **6** and **10** exhibited much lower oxidation potentials compared with **5** and **8**. As reported

TABLE 1. Oxidation Potentials of *meso*-Alkyl-, *meso*-Ester-, and *meso*-Aryl-Substituted Porphyrins

compd	E_{OX1}	E_{OX2}	ΔE
Zn-4	0.19		
5	0.17	0.34	0.17
6	−0.23	0.09	0.32
Zn-7	0.26		
8	0.19	0.37	0.18
10	−0.16	−0.25	0.14
11	0.38		
12	0.21	0.33	0.12
13	−0.02	0.45	0.47

previously, the first one-electron oxidation potentials in the directly linked diporphyrins **5**, **6**, **8**, **10**, **12**, and **13** are split, due to the influences of electronic interaction and first generated cationic charge that retards second oxidation. Here we define the value of potential difference, $\Delta E = E_{\text{ox1}} - E_{\text{ox2}}$, where E_{ox1} and E_{ox2} represent split potentials for the first oxidation. Interestingly, the ΔE values of **5** and **8** were slightly larger than that of **12**, while the ΔE values of **6** and **10** were smaller than that of **13**, indicating that the electronic interactions of *meso-meso* linked diporphyrin and triply linked diporphyrins are differently influenced by the substituents at the *meso*-positions.

In conclusion, *meso*-alkyl-substituted *meso-meso* linked diporphyrins and triply linked diporphyrins were synthesized from trialkyl-substituted porphyrin. The ester-bearing porphyrin dimers are useful and versatile substrates, allowing the transformation into more soluble substrates via the effective transesterification. Electronic interactions between the porphyrins are differently influenced by *meso*-aryl and *meso*-alkyl substituents. *meso*-Hexahexyl-substituted triply linked diporphyrin **6** is practically insoluble in CHCl_3 and indeed shows a high aggregation tendency.

Acknowledgment. This work was partly supported by Grant-in-Aid from the Ministry of Education, Culture, Sports, Science and Technology, Japan and 21st Century COE on Kyoto University Alliance for Chemistry.

Supporting Information Available: Experimental procedures and characterization data including ^1H NMR spectra. This material is available free of charge via the Internet at <http://pubs.acs.org>.

JO0502192